Research Article

Journal of Environmental Nanotechnology

Valorization of Coal Ash Waste in AA6061-graphene Nanocomposites Towards Environmental Sustainability

S. Sathish[1*], S. Sundaraselvan[2], G. B. Sathishkumar[2] and M. Kumaresan[3]

[1]Department of Mechanical Engineering, Sri Ramakrishna Engineering College, Coimbatore, TN, India
[2]Department of Mechanical Engineering, Arasu Engineering College, Kumbakonam, TN, India
[3]Department of Chemistry, Nehru Institute of Technology, Coimbatore, TN, India
Received: 07.02.2026 Accepted: 25.03.2026 Published: 30.03.2026
*sathishresearch2012@gmail.com

ABSTRACT

AA6061-fly ash (FA)-graphene nanoplatelet (GNP) hybrid nanocomposites (HNCs) were stir cast using 2 wt.% GNP and 3-15 wt.% FA. Adding leftover FA as strengthening promotes sustainability and value. Density study showed that increasing FA reduced theoretical and experimental densities and increased porosity. The sample HNC4 (12 wt.% FA+2 wt.% GNP) had 13.372% (estimated) and 15.712% (experimental) density, lower than as-cast AA6061, but 71.193% higher porosity. Mechanical assessment demonstrated maximal strengthening for HNC4, with universal tensile strength (UTS), flexural strength, and micro-hardness improving 32.464%, 25.581%, and 32.609%, respectively. Ductility and impact strength reduced by 94.525% and 21.795%, demonstrating the strength-toughness balance. The insulating properties and contact phonon scattering of FA reduced thermal conductivity by 24.944%. Due to enhanced hardness and GNP-rich tribo-film development, moderate reinforcement levels lowered wear loss (WL) and coefficient of friction (CoF). The sample HNC5 (15 wt.% FA+2 wt.% GNP) showed marginal deterioration beyond the optimal composition (density decreased by 3.382%, porosity rose by 14.593%). For HNC5, UTS, flexural strength, and impact strength diminished by 2.837%, 1.713%, and 5.405%, while hardness elevated slightly (3.158%). There was 7.692% and 7.317% increase in WL and CoF, indicating reinforcement saturation, particle consolidation, and tribo-film destabilization. The sample HNC4 exhibited the best lightweight-mechanical performance ratio.

Keywords: Hybrid nanocomposite; Waste valorization; Tribology; Graphene nanoplatelet; AA6061; Fly ash.

1. INTRODUCTION

Metal matrix composites (MMCs) integrate the ductility and toughness of metallic matrices with strength, stiffness, and thermal endurance, making them a crucial class of innovative engineering materials. The choice of lightweight materials in aircraft, cars, and structural purposes has increased MMC research since weight reduction improves fuel efficiency, emissions, and performance (Ramakrishnan and Gopal, 2025). Aluminum-based composites are popular matrix materials due to their low density, high specific strength, corrosion resistance, and manufacturability. Aluminum has better oxidation resistance, thermal stability, processing complexity, and industrial adaptability than magnesium alloys, which have severe flammability and corrosion issues. Aluminum-based composites are a flexible and cost-effective way to produce lightweight, high-performance components for several engineering industries (Kar *et al.* 2024). Aluminum-based composites using fly ash (FA) and red mud have gained popularity for their environmental and technical benefits. Thermal power stations and alumina industries produce enormous amounts of trash that pose disposal and ecological issues. Their use as reinforcements improves waste valorization and sustainable manufacturing (Naib, 2026). Fly ash and red mud include hard ceramic ingredients (oxides of silicon, aluminum, and iron) that improve aluminum matrix stiffness, hardness, wear resistance, and thermal stability while lowering material cost and density. Their use therefore not only mitigates environmental impact but also enables the development of lightweight, cost-effective composites with improved functional performance, making them attractive for structural and tribological applications (Mathew and Kottur, 2025).

Yashpal *et al.* (2018) developed aluminum-based composites containing AA6061 as matrix, FA, and Al_2O_3 as strengthening agents, developed *via* stir casting. Adding FA enhances micro-hardness but lowers density. Microstructure of cast composite shows that reinforcements are well distributed. Composite strength can come from either particle reinforcing or dispersion strengthening. By utilizing solid-state procedures such as cryo milling, cold compaction, and hot extrusion, Vatansever *et al.* (2011) fabricated composites by

recycling AA6061 chips and incorporating FA particles. Compared to unreinforced AA6061, recycled composites have lower densities and electrical conductivities. Hardness and compressive strength were both improved in the recycled composites containing coarse granulated chips as compared to those containing fine granulated chips. Adding more FA to recovered composites with rough granulated chips reduced their compressive strength. By using compocasting, Barah *et al.* (2026) fabricated AA6061/FA composites with reinforcement ranging from 4 to 12 wt.%. Zener pinning and heterogeneous nucleation were responsible for the grain refinement, pore-free surfaces, and uniform FA dispersal. The maximum tensile strength increased from 140 to 249 MPa (+78%), and the microhardness increased from 55 HV (unreinforced AA6061) to 110 HV (FA 12 wt.%). Fractography showed mixed-mode fracture surfaces with unbroken and fragmented particles, suggesting substantial interfacial adhesion, and ductility dropped from 14% to 5%. Selvam *et al.* (2017) fabricated AA6061+FA composite using stir casting and evaluated the wear characteristics. Wear resistance was temperature independent and improved as FA particle concentration increased in the composite. Particles of FA showed thermodynamic stability by not decomposing even when subjected to extremely high temperatures. With the addition of FA, the aluminum-based composites exhibited reduced plastic deformation and cutting even at room temperature. Abrasion, oxidation, delamination, and adhesion are some of the factors that lead to wear. A significant influence on the wear pattern is the heat treatment.

Murmu *et al.* (2024) developed hybrid AA6061+SiC+FA composites *via* stir casting approach. The hybrid material with the least volumetric loss, measuring 0.96 g, was the MMC 78% Al6061+15% SiC+7% (sample 3) FA. When comparing all the measured compositions, the one with the greatest wear and volumetric losses was 90% Al6061+5% SiC+5% FA. Compared with the other samples, the hybrid MMC (sample 3) showed improved hardness properties with 60.49 HRH. Scratch testing revealed that hybrid MMC sample 3 had the best abrasion resistance out of all the samples. Kumar *et al.* (2024) developed AA6061+FA+graphite+magnesium composite using stir casting and performed wear tests. The optimized formulation including 6 wt.% FA showed the lowest wear rate during the test. Results from SEM showed that the matrix included a consistent amount of FA and Gr, which increased its resistance to wear. Composites with a greater FA content showed less plastic deformation and scratches, suggesting a lower wear rate and better wear resistance.

Nanofillers activate numerous nanoscales strengthening processes in aluminum-based composites, improving their mechanical and functional performance. Nanofillers including graphene, CNTs, nano clay, and nano-oxides boost load transfer efficiency, constrain dislocation motion, and refine grain, increasing strength, hardness, and durability against wear due to their large surface area and outstanding intrinsic qualities. Orowan looping, thermal mismatch-induced dislocation formation, and interfacial strengthening improved, while nanofiller uniformity increased thermal stability and fatigue resistance (Yadav *et al.* 2024). Additionally, nanofillers can reduce crack initiation and propagation by acting as effective barriers, thereby improving durability. Consequently, nanofiller-reinforced aluminum-based composites exhibit superior specific properties compared to conventional micro-reinforced systems, enabling their use in high-performance lightweight applications. Jayaseelan *et al.* (2022) reinforced graphene nanoplatelets (GNPs) in AA2024, AA6061, and AA7075 via powder metallurgy, the reinforcing particles had a uniform distribution. At 2 wt.% of graphene, aluminum alloys reach their maximum yield strength. According to reports, AA 7075 has performed better than competing alloys because of its unique alloy qualities. Indicative of a load transfer from matrix to reinforcement, graphene pulls and shreds.

Using hot extrusion process, Gowda *et al.* (2021) developed AA6061+GNP composites and both hardness and tensile strength increased significantly as the percentage of GNPs in the material increased. Due to the homogeneous dispersion of GNP and excellent interfacial connections across matrix and reinforcement, the produced composites exhibit an improvement in wear resistance with an upsurge in GNP content. The ductile fracture of AA6061 changes into a brittle fracture in the manufactured composite, according to the fracture analysis. Sekhar *et al.* (2022) addressed the fabrication and characterization of Al7075-GNP composite in semi-solid stir casting. The material's hardness, tensile and compressive strength, and elongation strength all decline as the stirring temperatures increase. There was an increase in hardness number, compression strength, and tensile strength after GNP reinforcement. Lazarova *et al.* (2022) combined pure aluminium powder and GNP to develop composites in powder metallurgy and subjected to annealing. Nano-sized carbides of the Al_4C_3 type measuring 20 nm in size were accomplished. Aluminum matrix and GNPs make up the microstructure of extruded samples, which provide them the best strength qualities and microhardness. With microstructure components including nano-sized carbides, aluminum matrix, and GNPs, extruded and annealed samples exhibit decreased microhardness and strength qualities. This is because annealing lowers the material's strength even further. Hybrid nanocomposites (HNCs) of aluminum matrices are unique because they synergistically combine reinforcements of different length scales and functionalities to achieve property combinations unattainable with single fillers. The presence of micro-scale particles and nanoscale compounds activates several strengthening processes,

improves load transmission, grain refinement, and wear resistance. Nanoscale fillers reduce interfacial defects and promote tribofilm formation, balancing mechanical, thermal, and tribological performance in micro-reinforcements. This multi-scale reinforcing method allows for lightweight, high-performance aluminum composite architecture (Patel and Shi, 2025).

Most prior studies on AA6061-FA systems focus on micro-scale FA addition alone, while GNP-based AA6061 composites are typically investigated separately at low GNP contents due to dispersion and wettability challenges. Therefore, the combined influence of waste FA (0-15 wt.%) with a fixed GNP nanofiller level (2 wt.%) on simultaneous mechanical and dry-sliding tribological response remains insufficiently reported. There is a clear gap in establishing an optimum FA fraction under a constant nano-lubricious/strengthening GNP network. Correlating density-porosity evolution with strength, hardness, and wear transitions across the FA range is needed. Also, explaining the dominant wear mechanisms as the reinforcement balance shifts from strengthening-dominated to defect/porosity-dominated regimes is performed, which is the novelty of this study. The present work systematically maps the mechanical and tribological trends of AA6061 by varying FA from 0 to 15 wt.% while maintaining graphene at 2 wt.% (hybrid micro-nano reinforcement). This study links property changes to dispersion/porosity effects and wear-tribofilm mechanisms to identify an optimum composition for lightweight, eco-friendly, wear-resistant AA6061 hybrid nanocomposites, which is innovative.

2. MATERIALS AND METHODS

2.1 Matrix and Reinforcements

AA6061 is a widely used Al-Mg-Si alloy valued for its favorable strength-to-weight ratio, good corrosion resistance, and adequate thermal conductivity, making it suitable for structural and thermal management applications. AA6061 has a density of about 2.71 g/cc, thermal conductivity of 170 W/mK, and good mechanical strength (UTS of 300 MPa, YS of 250 MPa in T6 condition). Its balanced combination of lightweight, strength, thermal performance, and corrosion resistance makes it widely used in aerospace, automotive, heat exchanger, and structural applications (Yuvaraj *et al.* 2023). The EDX spectrum of the AA6061 alloy considered in this work is provided in Fig. 1.

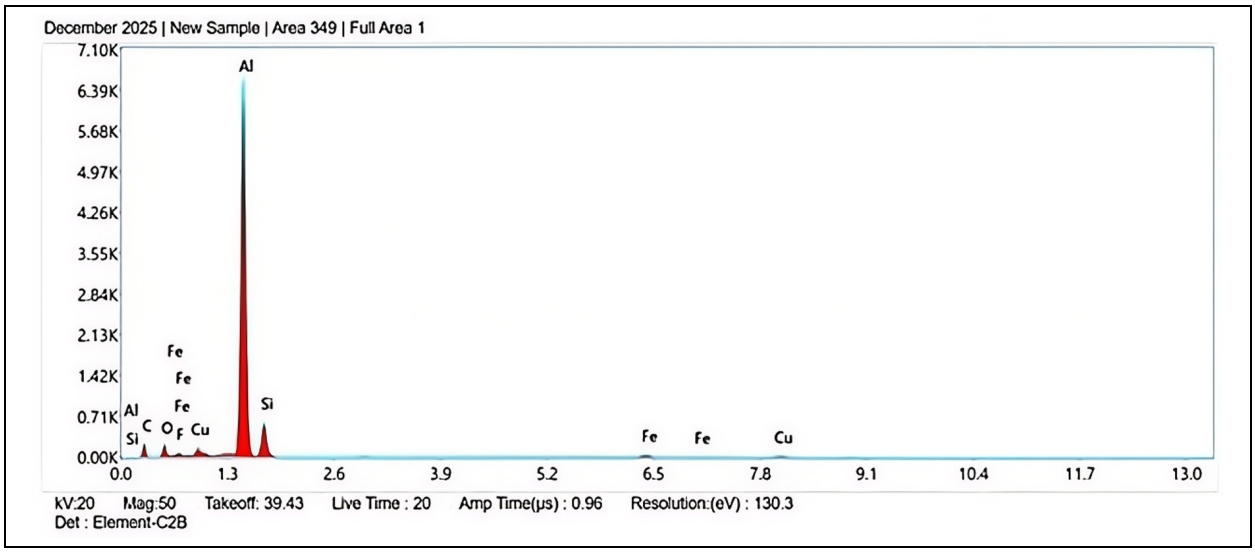


Fig. 1: EDX spectrum of AA6061 showing elements present

Fly ash, a thermal power plant by-product abundant in silica and alumina, serves as a cost-effective and environmentally friendly reinforcement. It improves stiffness, hardness, and thermal stability *via* dispersion strengthening and transferring loads, while also facilitating waste valorization. It generally exhibits a density of 1.3 g/cc and a modest thermal conductivity of 0.25 W/mK, which provides effective thermal insulation properties. Due to its elevated silica-alumina content, FA demonstrates significant hardness and stiffness; however, it is brittle. This property renders it appropriate for incorporation into construction materials and as a viable reinforcement in metal and polymer matrix composites, enhancing stiffness and thermal stability while repurposing industrial waste (Singh *et al.* 2025).

This research investigates FA particulates ranging from 40 to 80 µm. Graphene nanoplatelets due to their high elastic modulus, tensile strength, and thermal conductivity are an effective nanoscale reinforcement that enhances interfacial bonding, and limits dislocation motion by refining microstructure. They possess an

intrinsic density of 2.3 g/cc, a thickness ranging from 2 to 4 nm, and exhibit thermal conductivity of 3000 W/mK. They are favored as nano-reinforcements in lightweight structural nanocomposites, thermally optimized materials, technological devices, and aeronautical applications due to their ability to enhance strength and facilitate heat dissipation at low loadings (Lin *et al.* 2025). The combination of FA and GNPs within the AA6061 matrix provides multiscale reinforcement, where FA contributes to macro-scale load bearing and thermal resistance, while GNPs enhance nanoscale strength and facilitate heat transport channels. This synergy enhances mechanical performance, thermal stability, and expansion relative to monolithic AA6061, while promoting sustainable material development *via* industrial waste and advanced nanotechnology.

2.2 Ultrasonic Assisted Stir Casting

Ultrasonic-aided stir casting was utilized for developing the HNCs. A resistance furnace was utilized to melt and superheat AA6061 alloy to 780 ℃. Subsequently, degassing was performed using hexachloroethane to remove dissolved hydrogen and non-metallic impurities, thereby minimizing gas entrapment. Preheating FA and GNPs at 450 ℃ eliminated moisture and enhanced wettability prior to their incorporation into the molten alloy. The mechanical churning process, utilizing a graphite-coated impeller at 600 rpm for a duration of 10 minutes, facilitated the distribution of reinforcement and minimized flaws induced by vortices (Kumar *et al.* 2025). A 20 kHz ultrasonic probe (1.5 kW) submerged in the melt for 5 minutes in pulsed mode facilitated cavitation-assisted GNP deagglomeration, particle-matrix wetting, and refinement of grain structure. After pouring the homogenized melt into a warmed steel mould (200 ℃), it solidified under controlled environment to develop defect-minimized HNCs castings for subsequent testing.

2.3 Characterization Methods

The HNCs were characterized according to ASTM standards for consistency and comparability. For capturing SEM images, mounting the samples with bakelite powder allowed them to be polished for the microstructural investigation. After that, SiC sheets with grit levels ranging from 1200-1600 µm were utilized to polish the mounted samples. Lastly, mirror polishing was done using diamond paste (1 µm size). The tensile characteristics were evaluated in accordance with ASTM E8 standards, employing universal apparatus for testing at ambient temperature and a strain rate of 1×10^{-3} s^{-1}. The span-to-depth ratio for ASTM D790 3-point bending flexural strength measurements was 16:1 (Sankarasabapathi *et al.* 2025). The Izod technique, in accordance with ASTM E23, employed notched specimens and a standard pendulum impact tester to assess impact strength. Micro-Vickers hardness was assessed following ASTM E384, utilizing a test load of 300 gf (HV0.3) and a dwell time of 15 seconds. The results averaged over five indentations to minimize variability (Prakash *et al.* 2023). Porosity was estimated from the variance among theoretical and experimental densities using Archimedes principle and the reverse rule of mixtures, as per ASTM B962. According to the ASTM D3850 procedure, the thermal conductivity was evaluated by Lee's Disc method within a temperature span of 0 to 250 ℃, with 5 $MJ/m^3/K$ capacity specific heat, and thermal conductivity spanning from 0.005 to 1800 W/m/K (Ogunbiyi *et al.* 2025). Dry sliding wear behaviour was assessed using a pin-on-disc apparatus following ASTM G99, under controlled 10 N load, sliding speed of 2 m/s, and 500 m distance, as wear loss (WL) and friction coefficient (CoF) were continuously monitored (Jeffrey *et al.* 2025). The HNCs were fabricated with different compositions as shown in Table 1.

Table 1. Composition of HNCs

Notation	AA6061 %	FA %	GNPs %
As cast	100	0	0
HNC1	95	3	2
HNC2	92	6	2
HNC3	89	9	2
HNC4	86	12	2
HNC5	83	15	2

3. RESULTS AND DISCUSSION

After fabricating the HNCs, the samples were subjected to characterization techniques. The lightweight characteristics of the HNCs were evaluated through density measurement. The results as presented in Fig. 2 show a clear inverse trend between experimental density and porosity as the reinforcement level increases from as cast to HNC5. This is primarily driven by density contrast and defect formation, hence, replacing part of the matrix with FA and GNPs progressively reduces the rule-of-mixtures density. So, HNC1 to HNC5 naturally showed lower measured density. At the same time, the increasing reinforcement fraction raises the melt's effective viscosity and the number of particle-matrix interfaces, which makes it easier to trap gases and form voids during stirring/solidification (Vijaya *et al.* 2026). Fly ash particles that are often porous/irregular and GNPs having high surface area, and tendency to agglomerate can exhibit limited wettability with Al if local mixing or interfacial bonding is insufficient, leading to particle clustering, interfacial debonding, and micro-shrinkage cavities around poorly wetted regions (Senthilkumar, 2024). As the FA content rises, these effects intensify and more clusters and more sites for pore nucleation arises so the % porosity increases, which further lowers the

experimental density beyond what composition alone would predict.

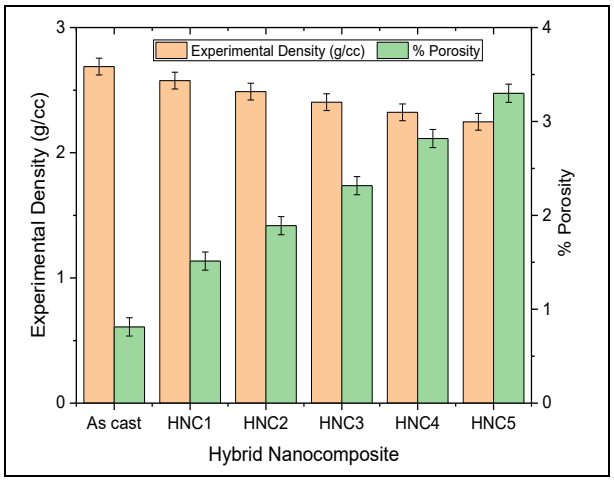


Fig. 2: Experimental density and porosity of HNCs

Fig. 3 presents the theoretical density of the HNCs based on the inverse rule of mixtures as weight fraction is considered. The theoretical density of the HNC decreases progressively with increasing FA content from HNC1 to HNC5. This reduction is mainly due to the much lower density of FA compared with AA6061. So, replacing part of the aluminium matrix with FA lowers the overall mass per unit volume. The contribution of GNPs to density change is relatively small because its density is closer to that of AA6061 and its weight fraction is constant. Hence, the observed decline in theoretical density is predominantly governed by the increasing proportion of low-density FA reinforcement (Sundaraselvan *et al.* 2025).

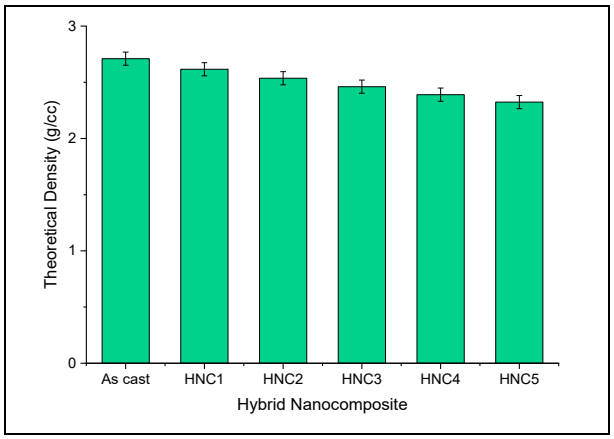


Fig. 3: Theoretical density of HNCs

The UTS of the HNCs increases progressively from the as-cast alloy to the reinforced compositions, reaching a maximum around the intermediate reinforcement levels (typically HNC4), while ductility correspondingly decreases as displayed in Fig. 4. Effective load transmission from the ductile matrix to the stiff FA fragments and high-strength GNPs, dispersion strengthening, thermal expansion mismatch-induced dislocations, and plastic flow restriction increase strength (Wang *et al.* 2019). As reinforcement ratio increases, ductility decreases because hard, non-deforming particles restrict matrix plasticity and encourage early cracking. Higher FA fractions (HNC5) saturate or diminish the strengthening effect due to particle agglomeration, greater porosity, and poorer interfacial bonding, which function as stress concentrators and cause premature failure. Grain refining increases grain boundary resistance (Kumar *et al.* 2025).

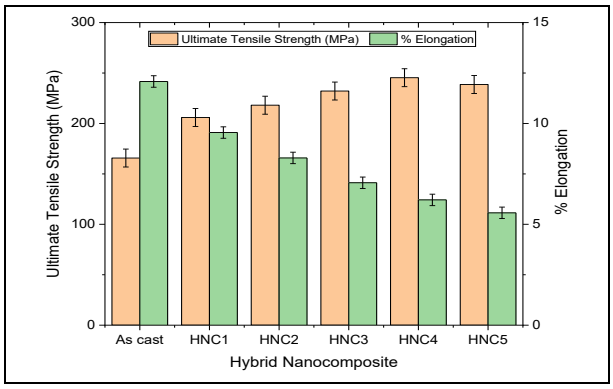


Fig. 4: UTS and ductility of HNCs

Tensile fracture SEM (Fig. 5) shows a reinforcement-induced fracture behaviour change. As-cast AA6061 (Fig. 5a) has pronounced dimples and micro void coalescence, indicating ductile fracture caused by considerable aluminium matrix plastic deformation. In HNC1 (Fig. 5b) and HNC2 (Fig. 5c), the fracture surfaces exhibit a mixed mode reaction characterized by the presence of dimples alongside flatter cleavage-like patches, indicating a quasi-brittle fracture (Huang *et al.* 2023). Fly ash particles and GNPs obstruct matrix flow and elevate localized stress, resulting in this shift. The sample HNC3 (Fig. 5d) exhibits heterogeneous fracture characteristics, such as particle-matrix breaking down, microcracks, and small dimples, indicating the initiation of reinforcing boundary cracks. This suggests strengthening through load transfer from matrix to hard FA particles and stiff GNPs, dislocation generation due to thermal-expansion mismatch, and local crack pinning/deflection (Harichandran and Selvakumar, 2018). The sample HNC4 (Fig. 5e) exhibits cleavage surfaces, particle pull-out sites, and interfacial spaces, which suggest diminished plasticity and enhanced crack propagation across weak interfaces attributed to elevated porosity and particle aggregation at high FA content. This is strong microstructural evidence of uniform reinforcement distribution, effective interfacial bonding, better stress transfer, crack bridging and longer crack path warpage, which together produce superior strengthening. The sample HNC5 (Fig. 5f) exhibits high agglomeration effects, separated particles, and interconnected voids, indicating that excessive

reinforcement leads to premature failure through interfacial degradation and crack linkage (Lyu *et al.* 2021).

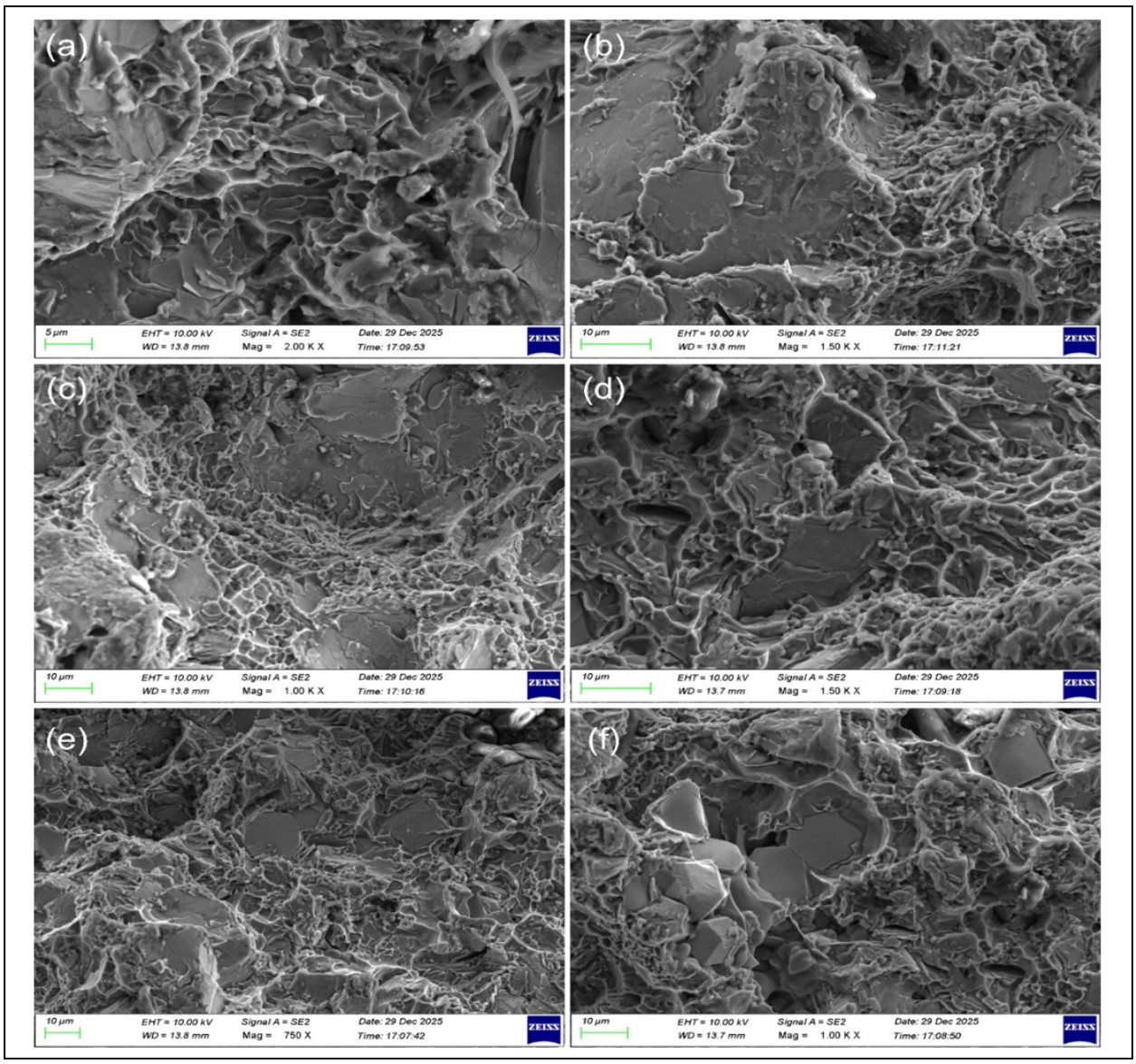


Fig. 5: SEM fractography of tensile samples (a) as cast (b) HNC1 (c) HNC2 (d) HNC3 (e) HNC4 and (f) HNC5

Fig. 6 demonstrates that the impact strength of HNCs declines progressively, whereas their flexural strength enhances with the addition of reinforcing content. The rigidity of the composite, along with the presence of hard FA particles and high-modulus GNPs, enhances resistance to bending deformation and restricts matrix plasticity, thereby increasing flexural strength. Enhanced load transfer, dispersion strengthening, and restricted dislocation motion diminish the initiation and propagation of fractures under flexural stress (Devendran and Lakshmi, 2025). Brittle ceramic components and limited matrix plastic deformation diminish energy absorption and impact strength. Increased reinforcing content leads to stress concentrations, particle clustering, and the development of micro voids, which can initiate cracks under sudden loading and diminish toughness. Reinforcement enhances bending resistance while reducing impact energy absorption due to increased brittleness and susceptibility to imperfections (Anbarasan *et al.* 2025).

Fig. 7 illustrates that reinforcing enhances HNC micro-hardness while decreasing thermal conductivity. Hard FA particles and high-stiffness GNPs prevent localized plastic deformation, dislocation motion, and indentation, improving hardness. Uniform particle dispersion, thermal mismatch dislocation strengthening, and matrix constraint effects increase hardness (Rubi *et al.* 2024). Because FA has innately low thermal

conductivity and functions as a heat-flow barrier in the aluminium matrix, thermal conductivity decreases. More interfaces, phonon scattering sites, and micro-defects reduce heat transport as reinforcement content increases. Graphene nanoplatelets exhibit exceptionally high electrical conductivity; however, their low and fixed content limits their ability to effectively offset the insulating effect of fly ash. The composite's surface hardness improves while heat conduction decreases (Saboori *et al.* 2017).

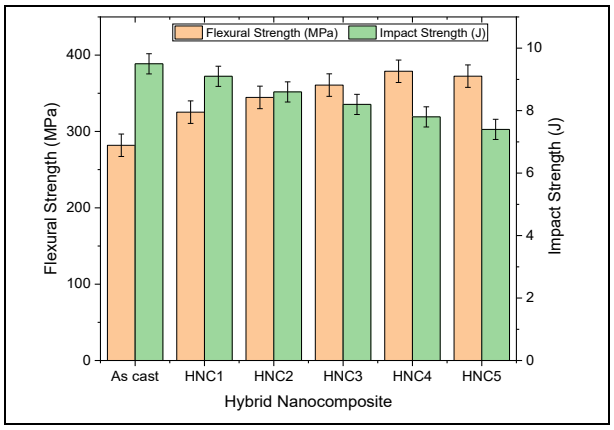


Fig. 6: HNCs impact and flexural strength

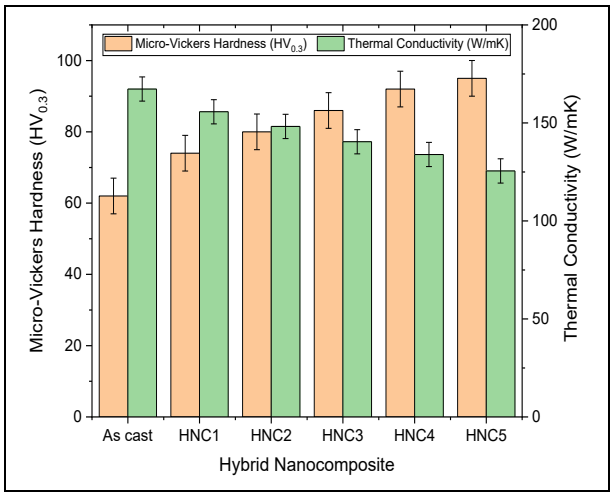


Fig. 7: HNCs hardness and heat conductivity

Tribological data (Fig. 8) demonstrate that reinforcement reduces WL significantly, whereas CoF declines at moderate reinforcement concentrations and varies somewhat at higher concentrations. The occurrence of hard FA particles is primarily responsible for the increased wear resistance, which enhance surface hardness and load-bearing capacity, thereby limiting severe plastic deformation and material removal during sliding (Jagadeeswaran *et al.* 2025). Graphene nanoplatelets play a crucial role by forming a thin lubricating tribo-film at the contact interface, which reduces direct metal-to-metal contact, shear stresses, and adhesive wear. The combined effect of hard ceramic reinforcement and solid lubrication promotes a transition from severe adhesive wear to milder abrasive or oxidative wear mechanisms. At higher reinforcement fractions, slight fluctuations in friction and wear behaviour can occur due to particle agglomeration, interfacial debonding, and increased porosity, which act as stress concentrators and may disrupt the stability of the lubricating film (Lu *et al.* 2021).

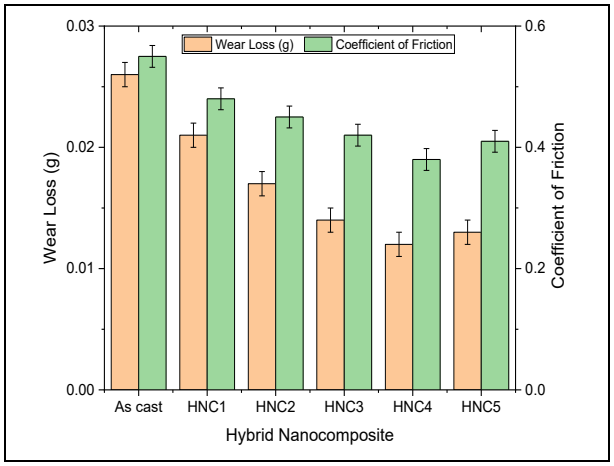


Fig. 8: Tribological performance of HNCs

Compared with the as-cast AA6061, HNC4 shows an overall lightweight strengthened but less ductile response. The theoretical and experimental densities drop by 133.372-15.712%, while porosity rises markedly (71.193%), indicating that the low-density FA dominates the mass reduction but the higher reinforcement level also promotes pore formation due to higher melt viscosity, gas entrapment and interfacial voids. Despite this porosity, strength-related properties improve. The UTS and flexural strength increase by 32.464% and 25.581%, and micro-hardness rises by 32.609% mainly due to load transfer, dispersion/dislocation strengthening and matrix constraint from FA and GNP. In parallel, ductility and impact strength decrease (94.525% and 21.795%) because hard particles reduce plastic deformation and porosity/particle clusters act as crack initiators under tensile/impact loading. Thermal conductivity decreases (24.944%) because FA interrupts heat flow and added interfaces/defects increase scattering. When moving from HNC4 to HNC5, most properties slightly deteriorate, density falls a bit further (3.382%), porosity increases (14.593%), and UTS/flexural/impact drop (2.837%, 1.713%, 5.405%), consistent with reinforcement saturation where extra FA increases agglomeration and porosity, weakening interfacial integrity and accelerating crack initiation (Razzaq *et al.* 2017). At the same time, micro-hardness still increases slightly (3.158%) due to the higher fraction of hard phases, but tribology worsens WL and friction rise (7.692% and 7.317%) likely because excessive FA, porosity destabilizes the graphene-rich tribo-film and

promotes particle pull-out, producing third-body abrasion and higher interfacial shear (Swain *et al.* 2025).

4. CONCLUSION

In this study, ultrasonic aided stir casting was adopted for fabricating HNCs made of AA6061, FA, and GNPs. The results show that FA and GNPs modify AA6061 characteristics to yield a lightweight, stronger hybrid nanocomposite. Increasing FA percentage reduced density, with HNC4 decreasing 13.372% (theoretical) and 15.712% (experimental) from the as-cast alloy. The higher decline in experimental density increases porosity (71.193%) due to melt viscosity, gas trapping, and interfacial void formation. The UTS, flexural strength, and micro-hardness enhanced 32.464%, 25.581%, and 32.609% for HNC4, optimizing mechanical performance. These improvements are due to synergistic strengthening processes such load transmission, dispersion strengthening, thermal mismatch dislocation strengthening, and grain size reduction, with GNPs inhibiting dislocation motion. Ductility and impact strength decreased by 94.525% and 21.795% due to hard reinforcements and porosity reducing matrix plasticity and stress concentration. The insulating properties and contact scattering of fly ash reduced thermal conductivity by 24.944%. At moderate reinforcement levels, hardness and a GNP-rich lubricating tribo-film lowered WL and CoF, improving tribological behavior. The sample HNC5 showed reinforcement saturation, agglomeration, and defect sensitivity, with strength decreases and WL (7.692%) and CoF (7.317%) increases.

The developed HNCs have strong potential in automotive, aerospace, railway, marine, defense, and lightweight structural components, especially for parts requiring high specific strength, dimensional stability, thermal resistance, and reduced weight, such as brackets, housings, panels, pistons, connecting elements, and heat-dissipating components. Future work can focus on corrosion, fatigue, impact, creep, and high-temperature performance, along with machinability, weldability, tribo-corrosion, thermal/electrical behaviour, and recyclability studies, and optimization of GNP dispersion.

FUNDING

This research received no specific grant from any funding agency in the public, commercial, or not-for-profit sectors.

CONFLICTS OF INTEREST

The authors declare that there is no conflict of interest.

COPYRIGHT

This article is an open-access article distributed under the terms and conditions of the Creative Commons Attribution (CC BY) license (http://creativecommons.org/licenses/by/4.0/).

REFERENCES

Anbarasan, M., Perumal, G., Ponnuvel, S. and Senthilkumar, N., Synergistic Reinforcement of Aluminium Nanocomposites with SiC and Montmorillonite Nanoclay: Mechanical, Tribological and Corrosion Insights, *J. Mater. Eng. Perform*., (2025). https://doi.org/10.1007/s11665-025-12593-5

Barah, O. O., Bori, I., Otaru, A. J. and Zaid, Z. A. A. A., Processing Optimization of Sustainable AA6061–Fly Ash Composites by Compocasting, *ACS Omega*, 11(4), 6647–6656 (2026). https://doi.org/10.1021/acsomega.5c11742

Devendran, N. and Lakshmi, T. S., Investigation on the Physical and Mechanical Properties of Banana/Ramie Hybrid Composites Reinforced with Graphene Oxide Nanoparticles, *J. Environ. Nanotechnol.,* 14(3), 193–204 (2025). https://doi.org/10.13074/jent.2025.09.2531639

Gowda, B. N. Y., Haseebuddin, M. R., Pal, B. and Keshavamurthy, R., Mechanical and wear behaviour of graphite nano filler reinforced Al 6061 composites, *Mater. Today Proc.,* 46, 4504–4509 (2021). https://doi.org/10.1016/j.matpr.2020.09.690

Harichandran, R. and Selvakumar, N., Microstructure and mechanical characterization of (B4C+ h-BN)/Al hybrid nanocomposites processed by ultrasound assisted casting, *Int. J. Mech. Sci.,* 144, 814–826 (2018). https://doi.org/10.1016/j.ijmecsci.2017.08.039

Huang, Y. -H., Yang, F. -X., Wang, N., Zhu, M. -L. and Xuan, F. -Z., Improvement of stress corrosion cracking resistance by low cycle fatigue of a CrNiMoV steel, *Npj Mater. Degrad.,* 7, 58 (2023). https://doi.org/10.1038/s41529-023-00372-3

Jagadeeswaran, K. and Chelladurai, S. J. S., Evaluation of mechanical and wear properties of LM24/fly ash/titanium diboride hybrid metal matrix composites using stir casting, *Part. Sci. Technol.,* 43, 338–356 (2025). https://doi.org/10.1080/02726351.2025.2456596

Jayaseelan, J., Pazhani, A., Michael, A. X., Paulchamy, J., Batako, A. and Guruswamy, P. K. H., Characterization Studies on Graphene-Aluminium Nano Composites for Aerospace Launch Vehicle External Fuel Tank Structural Application, *Mater.,* 15(17), 5907 (2022). https://doi.org/10.3390/ma15175907

Jeffrey, J. A., Sivaraman, V., Kumar, S. S., Srinivasan, D., Joshika, S., Nithish, J. and Yuvaraj, R., Lokesh T., Evaluating the Material Performance of AZ91 Reinforced with 3 wt. % of Nano SiC and Micro B4C Through Stir Casting, *J. Environ. Nanotechnol*., 14(3), 371–378 (2025). https://doi.org/10.13074/jent.2025.09.2531601

Kar, A., Sharma, A. and Kumar, S., A Critical Review on Recent Advancements in Aluminium-Based Metal Matrix Composites, *Cryst.,* 14(5), 412 (2024). https://doi.org/10.3390/cryst14050412

Kumar, A., Barathiraja, K., Senthil, R., Stephena, E., Jeffrey, A. J., Kumar, D. V. and Kumar, S. S., Effect of Nano-SiO2 on the Mechanical Properties of AA6061 Stir-cast Composites, *J. Environ. Nanotechnol.,* 14(4), 113–119 (2025). https://doi.org/10.13074/jent.2025.12.2541910

Kumar, H., Prasad, R., Kumar, P., Sushma, I. S. P., Yelamasetti, B., Shelare, S., Sharma, S., Ismail, A. I. and Lozanovic, J., Synergistic mechanisms of fly ash reinforcement on the mechanical characteristics, deformation behaviour, grain refinement, and grain boundary in friction stir processed copper matrix composites, *J. Mater. Res. Technol.,* 36, 9831–9839 (2025). https://doi.org/10.1016/j.jmrt.2025.05.141

Kumar, R., Bairwa, K. N., Vemanaboina, H., Naidu, B. V., Shoush, K. A., Pushkarna, M., Tuka, M. B. and Ghoneim, S. S., Enhancing wear resistance of aluminum 6061 composites with fly ash: A sustainable approach for industrial applications, *Adv. Mech. Eng.,* 16(10), 290913 (2024). https://doi.org/10.1177/16878132241290913

Lazarova, R., Mourdjeva, Y., Nihtianova, D., Stefanov, G. and Petkov, V., Fabrication and Characterization of Aluminum-Graphene Nano-Platelets—Nano-Sized Al4C3 Composite, *Metals,* 12(12), 2057 (2022). https://doi.org/10.3390/met12122057

Lin, F., Ren, M., Zhu, L., Jia, F. and Jiang, Z., Graphene-reinforced aluminium matrix nanocomposites: Fabrication, properties and applications, *Adv. Nanocompos.,* 2, 59–85 (2025). https://doi.org/10.1016/j.adna.2024.12.001

Lu, X., Zhang, Y., Xiao, S., Lu, Y., Meng, D., Qin, W. and Li, J., Tribological behavior and mechanism of high proportion of ceramic particles reinforced Al composite, *J. Mater. Res. Technol.,* 15, 4931–4939 (2021). https://doi.org/10.1016/j.jmrt.2021.10.091

Lyu, S., Wang, Y., Han, H., Ding, C., Li, D., Wang, J. -K, Zhang, J., Huang, J., Sun, D. and Yu, P., Microstructure characterization and mechanical properties of Al-matrix composites reinforced by artificially-cultured diatom frustules, *Mater. Des.,* 206, 109755 (2021). https://doi.org/10.1016/j.matdes.2021.109755

Mathew, G. and Kottur, V. K., A review on the reinforcement of aluminium composites using industrial waste materials: Enhancing mechanical properties and tribological performance, *Next Mater*., 9, 101356 (2025). https://doi.org/10.1016/j.nxmate.2025.101356

Murmu, S. K., Chattopadhayaya, S., Cep, R., Kumar, A., Kumar, A., Mahato, S. K., Kumar, A., Sethy, P. R. and Logesh, K., Exploring tribological properties in the design and manufacturing of metal matrix composites: an investigation into the AL6061-SiC-fly ASH alloy fabricated via stir casting process, *Front. Mater.,* 11, 1415907 (2024). https://doi.org/10.3389/fmats.2024.1415907

Naib, -Al. U. M. B., Industrial and agro-waste reinforcements in aluminum matrix composites: Toward sustainable materials development, *Total Environ. Eng.,* 6, 100064 (2026). https://doi.org/10.1016/j.teengi.2026.100064

Ogunbiyi, O., Jamiru, T. and Akinwande, A. A., Mechanical and wear characteristics of aluminium-7068-composites structurally modified with medium-entropy-alloy, *Mater. Today Commun.,* 42, 111169 (2025). https://doi.org/10.1016/j.mtcomm.2024.111169

Patel, S. K. and Shi, L., Recent Advances in Ceramic-Reinforced Aluminum Metal Matrix Composites: A Review, *Alloys,* 4(3), 18 (2025). https://doi.org/10.3390/alloys4030018

Prakash, J. U., Juliyana, S. J., Salunkhe, S., Gawade, R. S., Nasr, E. S. A. and Kamrani, A. K., Mechanical Characterization and Microstructural Analysis of Stir-Cast Aluminum Matrix Composites (LM_5/ZrO_2), *Cryst.,* 13(8), 1220 (2023). https://doi.org/10.3390/cryst13081220

Ramakrishnan, T. and Gopal P. M.., Fundamentals and Advances in Metal Matrix Composites, *Taylor Francis Grp.*, 2024-01-5231(2025). https://doi.org/10.1201/9781003499718

Razzaq, M. A., Majid, D. L., Ishak, M. R. and Basheer, U. M., Effect of Fly Ash Addition on the Physical and Mechanical Properties of AA6063 Alloy Reinforcement, *Metals,* 7(11), 477 (2017). https://doi.org/10.3390/met7110477

Rubi, C. S., Prakash, J. U., Juliyana, S. J., Čep, R., Salunkhe, S., Gawade, S. R. and Nasr, E. S. A., Multi-objective optimization of machining variables for wire-EDM of LM6/fly ash composite materials using grey relational analysis, *Sci. Eng. Compos. Mater.,* 31, 20240008 (2024). https://doi.org/10.1515/secm-2024-0008

Saboori, A., Pavese, M., Badini, C. and Fino, P., Microstructure and Thermal Conductivity of Al–Graphene Composites Fabricated by Powder Metallurgy and Hot Rolling Techniques, *Acta Metall. Sin.,* 30, 675–687 (2017). https://doi.org/10.1007/s40195-017-0579-2

Sankarasabapathi, S., Subramaniam, N., Velmurugan, and S. and Nelson, G. R. E., Exploring the mechanical and microstructural characterization of stir cast aluminum 8011 matrix hybrid composites, *Matéria (Rio de Janeiro),* 30, 0904 (2025). https://doi.org/10.1590/1517-7076-rmat-2024-0904

Sekhar, K. C., Surakasi, R., Roy, P., Rosy, P. J., Sreeja, T. K., Raja, S. and Chowdary, V. L., Mechanical Behavior of Aluminum and Graphene Nanopowder-Based Composites, *Int. J. Chem. Eng.,* 2022(1), 2224482 (2022). https://doi.org/10.1155/2022/2224482

Selvam, D. R. J., Dinaharan, I. and Mashinini, P. M., High temperature sliding wear behavior of AA6061/fly ash aluminum matrix composites prepared using compocasting process, *Tribol. – Mater., Surf. Interfaces,* 11(1), 39–46 (2017). https://doi.org/10.1080/17515831.2017.1299324

Senthilkumar, N., Characterization of Graphene and Titanium Carbide Reinforced Magnesium Alloy Composite for Transmission Housings in Automobile, *SAE Tech. Paper*, 2024-01-5231 (2024). https://doi.org/10.4271/2024-01-5231

Singh, M., Kumar, P., Dahiya, D., Punia, U. and Tyagi, A., Fly ash as a sustainable reinforcement in composite materials: a comprehensive review on enhancing mechanical properties for eco-friendly engineering, *Discov. Mater.,* 5, 210 (2025). https://doi.org/10.1007/s43939-025-00331-6

Sundaraselvan, S, Prasad, D. V. S. S. S. V., Dinesh, N. and Bharathi, M. R., Evaluating the Mechanical Features of Nano Alumina Reinforced Magnesium Alloy-fly Ash Nanocomposites, *J. Environ. Nanotechnol.,* 14(2), 96–104 (2025). https://doi.org/10.13074/jent.2025.06.2511393

Swain, S. R., Subramanya, R., Hatti, P., Murthy, K. N. and Thirugnanasambandam, A., Tribomechanical properties of developed aluminium hybrid composites reinforced with MWCNT, SiC, and coconut shell ash, *Next Mater.,* 9, 101028 (2025). https://doi.org/10.1016/j.nxmate.2025.101028

Vatansever, R., Mindivan, H. and Kayali, E. S., Fly Ash Particle Reinforced AA6061 Composites Produced by Recycling of Aluminum Chips and Fly Ash Particles, *Adv. Mat. Res.,* 324, 38–41 (2011). https://doi.org/10.4028/www.scientific.net/AMR.324

Vijaya, M., Dhoria, S. H., Miditana, V., Zubairuddin, M., Mohammad, A. and Tamboli, S., Enhancement of LM26 Aluminum Hybrid Composites Performance Through SiC and Graphite Reinforcements Using Predictive ANN Modeling, *Eng. Rep.,* 8(1), e70562 (2026). https://doi.org/10.1002/eng2.70562

Wang, J., Guo, L., Lin, W., Chen, J., Liu, C., Chen, S., Zhang, S. and Zhen, T., Effect of the graphene content on the microstructures and properties of graphene/aluminum composites, *New Carbon Mater.*, 34(3), 275–285 (2019). https://doi.org/10.1016/S1872-5805(19)60016-8

Yadav, V., Pal, D. and Poonia, A. K., Nanofillers as a potential key for shaping the future of the industries, *Hybrid Adv.,* 7, 100340 (2024). https://doi.org/10.1016/j.hybadv.2024.100340

Yashpal, Panwar, N., Goud, M. M. and Kant, S., Experimental investigation of AA6061-Al2O3-fly ash composite produced by using stir casting method, *Mater. Today Proc.,* 5(14), 28413–28419 (2018). https://doi.org/10.1016/j.matpr.2018.10.127

Yuvaraj, N., Koli, Y., Vedabouriswaran, G. and Issar, P., Mechanical and Tribological Properties of AA6061/SiC/Aloe Vera Powder Hybrid Al Composites Fabricated by Stir Casting, *Silicon,* 15, 2451–2465 (2023). https://doi.org/10.1007/s12633-022-02168-7